[PROC. OF JSCE No. 344/I-1 (Structural Eng./Earthquake Eng.) April 1984]

MULTIPLE EVENT ANALYSIS OF 1979 IMPERIAL VALLEY EARTHQUAKE USING DISTINCT PHASES IN NEAR-FIELD ACCELEROGRAMS*

*By Yozo FUJINO***, Takashi YOKOTA****
*Yoshihiro HAMAZAKI***** and Ryosuke INOUE******

An analysis of identifying the multiple rupture process of the 1979 Imperial Valley, California earthquake is made utilizing distinct phases in the near-field horizontal accelerograms. Two methods are employed in the identification of the distinct phases; one is the visual inspection method and the other the quantitative method. The location of the source corresponding to the distinct phases is determined using the S-wave travel time curve. It is found that the earthquake is a multiple event with three smaller events in the period of less than 1 to 2 seconds and that the main energy is released from a localized portion about 8 to 13 kilometers from the epicenter to northwest along the fault. The results are compared with the spatial dislocation model of this earthquake obtained by Hartzell and Helmberger[3].

1. INTRODUCTION

Many empirical formulas have been proposed to relate the parameters of strong-ground motions such as peak acceleration, duration and response spectra to the magnitude of the earthquake, the epicentral distance and the site soil conditions. These formulas are, however, obtained on the basis of the accelerograms recorded mostly in the intermediate or long epicentral distances and therefore they may not be applicable to predict the near-field strong motions.

Near-field ground motions from a large earthquake are of great concern in connection with aseismic design of civil engineering structures, but their nature has been little known owing to very limited number of near-field records available. Since occurrence of large earthquakes is sporadic and furthermore, not so many strong motion instruments have been installed near causative faults until recently, it is very difficult to gather near-field strong ground motion records.

In view of the importance of near-field strong motion records, the U.S. Geological Survey and some other organizations installed many strong-motion accelerographs near the Imperial fault, California in 1975 and received a rewarding result from the 1979 Imperial Valley earthquake[4]. In more than 30 stations, the accelerographs performed properly. These accelerograms contain the most comprehensive collections of near-field strong motion data ever recorded and offer an unprecedented opportunity to study characteristics of near-field strong motions and moreover, to investigate the relation between the source mechanism and the strong motions. Detailed studies regarding these topics would lead to a more reliable prediction model of near-field strong motion employing

* partly presented in Refs. 1 and 2

** Member of JSCE, Ph.D, Assoc. Professor, Dept. of Civil Eng., Univ. of Tokyo (Bunkyo-ku, Tokyo)
*** Dr. Sci., Seismologist, Meteorological Res. Institute, Japan Meterological Agency (Tsukuba Sci. City, Ibaraki)
**** Member of JSCE, M. Eng., Res. Engineer, Structural Eng. Lab., Kobe Steel Co. Ltd. (Amagasaki, Hyogo)
***** Member of JSCE, Dr. Eng., Res. Assoc., Dept. of Construction Eng., Univ. of Ibaraki (Hitachi, Ibaraki)

appropriate parameters.

The objective of this paper is to reveal the multiple rupture process of the 1979 Imperial Valley earthquake by identifying distinct phases in the accelerograms recorded in the Imperial Valley strong-motion network (California) and in the Northern Baja network (Mexico) and to study the source characteristics from the near-field strong-motions.

Recent seimological studies (for example Refs. 5)-8)) indicate that most large earthquakes are complex multiple events in the periods of ten to several tens of seconds. Trifunac and Brune[9] interpreted that the main shock of the 1940 Imperial Valley earthquake was a multiple event even in the periods of less than one second and stressed on the importance of the multipleness of the rupture process from the engineering viewpoint. Their interpretation is based on the visual inspection of the single accelerogram recorded at El Centro during that earthquake and therefore, seems to be somewhat uncertain as far as the uniqueness of the interpretation is concerned. Since more than 30 near-field accelerograms are available in the 1979 event, more reliable analysis of multiple event in this period range can be expected even though the same method is employed.

Approaches of multiple event analysis used in seismology can be divided into two : the distinct phase approach (Refs. 7)-9), 12)) and the waveform matching approach (Refs. 5), 6)). The distinct phase method is to identify distinct phases in seismograms and to determine the location of the sources which generate such distinct phases, clarifying the multipleness of an earthquake. On the other hand, the waveform matching method is to construct a multiple dislocation model such that the synthetic ground motion(s) computed by the model matches the recorded seismogram(s) as closely as possible. The distinct phase approach is employed in this study.

2. 1979 IMPERIAL VALLEY, CALIFORNIA EARTHQUAKE[3),4),10),11)]

The October 15, 1979 Imperial Valley earthquake occurred at the well-defined Imperial fault with the epicenter of 32.63° N, 115.33° W. The local magnitude M_L reported by USGS is 6.6. The earthquake was shallow and the motion of the fault was primarily right-lateral vertical strike-slip; in these respects this event is a typical one in Southern California. The rupture propagated from the epicenter to the northwest direction on the fault of approximately 35 km length. The rupture velocity is estimated to 2.5-2.7 km/s[3]. The 1979 event is comparable in size to the famous 1940 event (M_L=6.4) which occurred at the same fault with the opposite direction of rupture propagation.

In Fig. 1, the location of the accelerographs triggered by the 1979 earthquake as well as the location of the causative fault is shown. One can see that the accelerographs are installed in various azimuths and distances from the fault. It should be noted that more than ten of the accelerograms had absolute trigger timing with millisecond accuracy. At El Centro Array No. 7 and Bonds Corner stations, the maximum horizontal accelerations (after instrumental correction) exceeded 0.5 g (1 g=

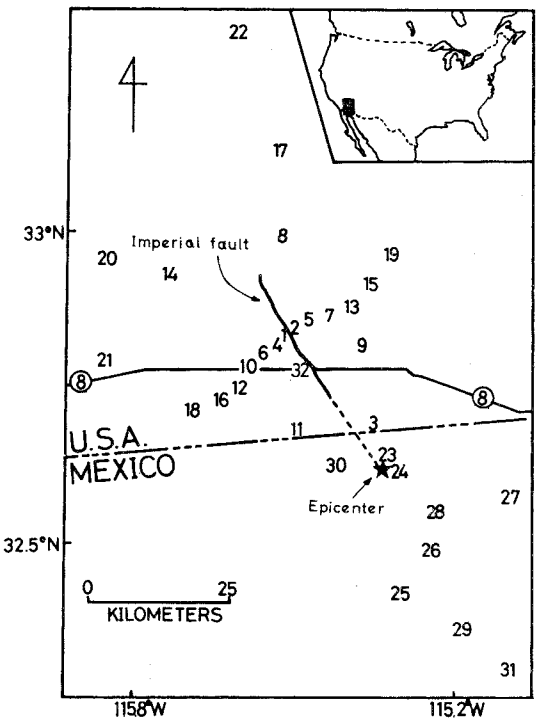

1 El Centro Array 7	12* El Centro Array 11	23 Aeropuetro
2* El Centro Array 6	13 El Centro Array 3	24 Agrarias
3* Bonds Corner	14 Parachute	25 Cerro Prieto
4* El Centro Array 8	15* El Centro Array 2	26 Chihuahua
5* El Centro Array 5	16* El Centro Array 12	27 Compuertas
6 El Centro Diff. Array	17 Calipatria	28 Cucapah
7* El Centro Array 4	18* El Centro Array 13	29 Delta
8* Brawley Airport	19* El Centro Array 1	30 Mexicali Sahop
9 Holtville	20 Superstition Mt.	31 Victoria
10 El Centro Array 10	21 Plaster City	32 Meloland
11* Calexico	22 Coachella	

*: absolute trigger time available

Fig. 1. Imperial valley strong-motion network and causative Imperial fault.

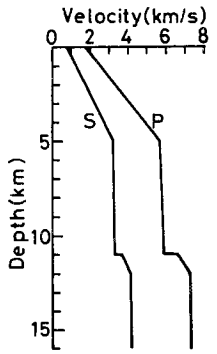

Fig. 2 Crustal model[13] : *S*- and *P*-wave velocity

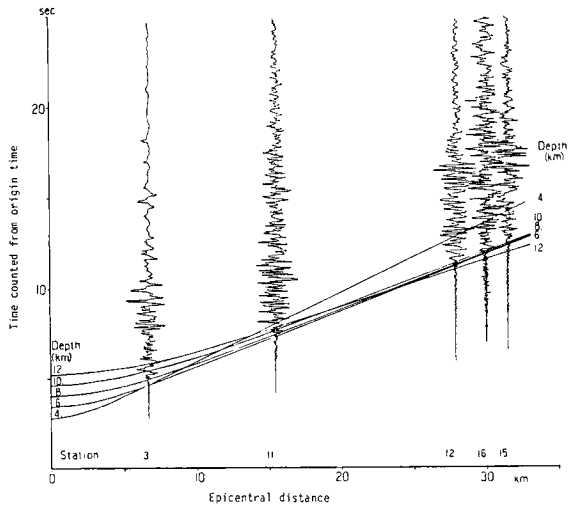

Fig. 3 Epicenter-oriented *S*-wave arrival time for various focal depths and recorded accelrograms.

980 cm/sec^2) and the maximum vertical acceleration at El Centro Array Station No. 6 was about 1.5 g[11].

The focal depth is herein examined. The S-wave travel time is calculated from the crustal model (Fig. 2) of this region proposed by Fuis *et al.*[13]. Fig. 3 shows the representative horizontal accelerograms with the absolute trigger timing and the epicenter-oriented S-wave arrival time curve for various values of the focal depth. The ordinate is the time after the origin time and the abscissa is the epicentral distance. It can been seen that the focal depth 12 km reported in Ref. 11) is not plausible for the record at the station near the epicenter. The focal depth of 7 to 8 km appears to be the most appropriate value and is used in the multiple event analysis which follows.

3. ANALYSIS

(1) Identification of Distinct Phase in Accelerograms

(a) Visual Inspection Method

Each distinct phase in a seismogram or an accelerogram can be defined as the phase following an abrupt change in the amplitude and (or) the phase of the recorded motion. It is not easy to identify the arrival times of distinct phases in accelerograms because the waveform of the accelerograms is generally very complex. The accelerograms contain motions of a wide range of frequency (0.2-25 Hz) and the contribution of each frequency motion to the total accelerograms fairly dependent on the frequency.

In this study the acceleration motions corrected from the original accelerograms under a standard routine[11] are resolved into various frequency range; the band-pass (or low-pass) filters of 2 Hz width (Chebychev filter with equiripple stopband[14]) are applied to each acceleration, and filtered accelerations having a relatively large amplitude as compared with the original acceleration are used in the analysis. Distinct phases are identified by careful visual inspection of these filtered accelerations selected; the individual authors independently identified distinct phase by their own judgment and with reference to the reconciled results the distinct phases are finally determined. Fig. 4 shows examples of accelerations, filtered accelerations and identified distinct phases marked out by arrows. For example, identification of the distinct phases in the records at Bonds Corner (Fig. 4 (a)) was made as follows. In the records, first *S*-wave arrival can be clearly seen around 2.5 sec and therefore we identified this as a distinct phase. After this phase, the amplitude is apparently dying out and sharp and abrupt change in amplitude can be seen around 5 sec. The 2-4 Hz filtered motion supports the existence of the second distinct phase. Its arrival time was determined with reference to the filtered motion. For other records, the same procedure is applied and filtered motions were referred whenever it was rather difficult to identify distinct phases and to

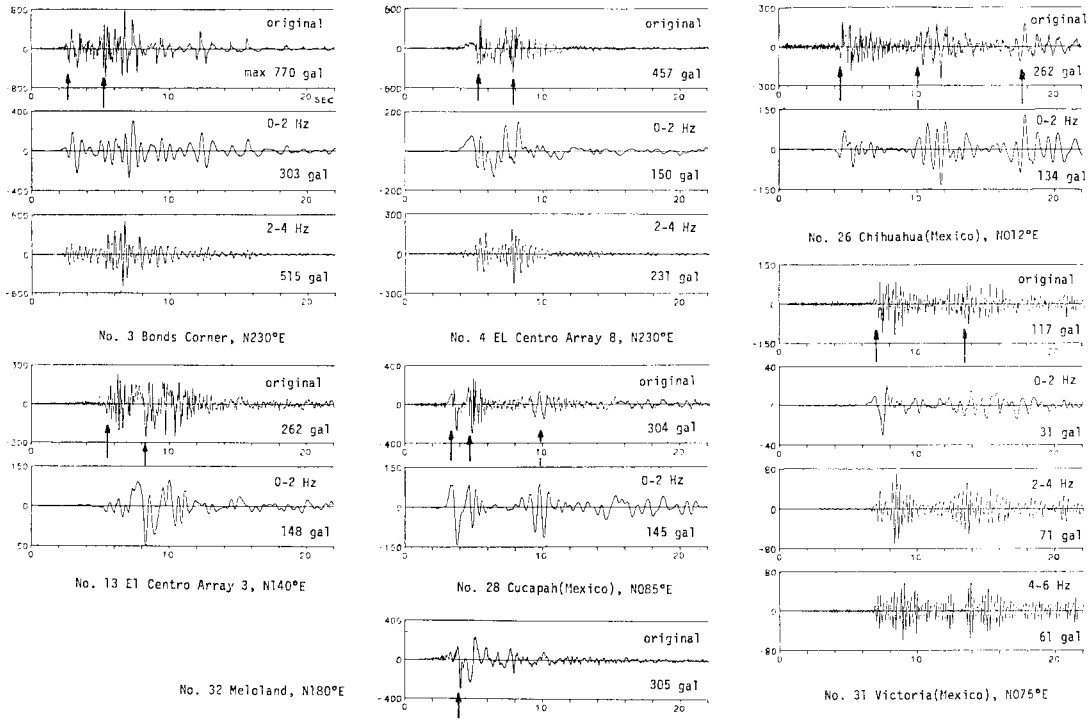

Fig. 4 Examples of acceleration motions, filtered motions and distinct phases identified by visual inspection.

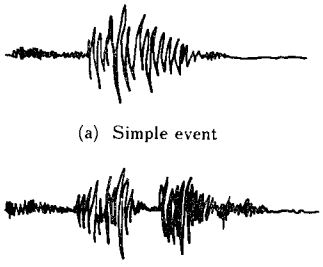

(a) Simple event

(b) Multiple event

Fig. 5 Ground motions.

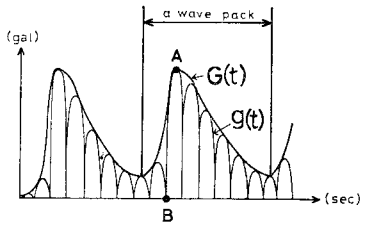

Fig. 6 Definition of arrival time of distinct phase by quantitative method

determine their arrival time from the original acceleration motions only. We can observe distinct phases more clearly in the records of the Mexican side ; this is probably due to the direction of the fault rupture.

Identifying distinct phases is done on the basis of authors' subjective judgment. To establish an objective criterion of the procedure is highly desired although this seems to be not easy from our experience. An attempt of the quantitative approach follows.

(b) Quantitative Method

The near-field ground motion due to a simple event generally takes a waveform as shown in Fig. 5 (a) ; its envelope has a single peak. In the case of a ground motion due to multiple event, there would exist multiple peaks in its envelope as shown in Fig. 5 (b). Each wave pack may be considered to correspond to individual event. Let $g(t)$ be defined as

$$g(t)=x^2(t)+y^2(t)$$

where $x(t)$ and $y(t)$ are the two horizontal acceleration components. Let $G(t)$ be the envelope of $g(t)$. In Fig. 6, the amplitude of $g(t)$ takes the local maximum at the point A. The point B where $g(t)$ takes the local minimum just

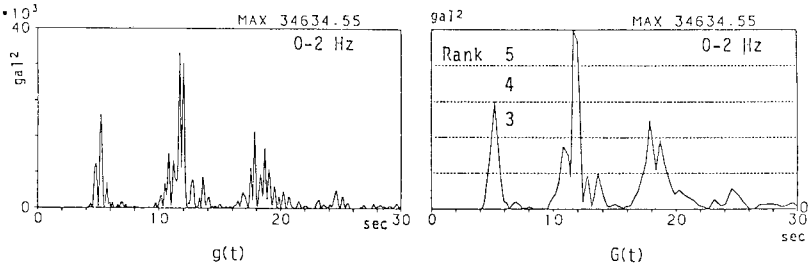

Fig. 7 An example of squared wave $g(t)$, its envelope $G(t)$ and rank of distinct phase

before the point A, idicates the arrival time of the large seismic wave energy. In this quantitative approach the point B is defined as the arrival of of the distinct phase generated by an event.

The original acceleration motions are resolved into three filtered motions with 0-2 Hz, 2-4 Hz and 4−6 Hz width, respectively. In each filtered motion, the arrival time of the distinct phases (point B) is determined according to the aforementioned criterion. The following rank is assigned to each identified distinct phase depending on the ratio r of the local maximum amplitude of $G(t)$ to the absolute maximum of $G(t)$; the rank is 3 for $r=0.4-0.6$, 4 for $r=0.6-0.8$, and 5 for $r=0.8-1.0$, respectively. Fig. 7 shows an example of $g(t)$ and $G(t)$. In this criterion, it is found that the S-wave arrival coming from the epicenter is not always identified as a distinct phase with a high rank even though it is clearly identified as a distinct phase by visual inspection. This is because the S-wave arrival from the epicenter is not necessarily large in amplitude. This is one of the drawbacks in this quantitative criterion. Another drawback may be that consecutive peaks of large amplitude due the same event are incorrectly judged to be due to two or more events. Further improvement is certainly needed.

(2) Determination of Location of Source Corresponding to Distinct Phase

Location of the source which corresponds to the distinct phase in each accelerogram is determined as follows. The causative fault of 38 km length is divided into small fault segments. The absolute arrival time T of the seismic wave due to the i-th fault segment in the station is given by

$$T_i = t_0 + \frac{L_i}{V_r} + t_i \quad \cdots\cdots (1)$$

where t_0=the origin time, L_i=the distance from the epicenter to the i-th fault segment along the fault, V_r=rupture velocity, t_i=travel time of S-wave from the i-th segment to the station.

In order to utilize the horizontal accelerograms having no absolute trigger timing, the trigger times are estimated using the S-wave travel curve. In this procedure it is assumed that the initial S-wave arrival seen in the

Table. 1 Trigger time minus origin time ($T-O$ time) estimated from initial S-wave motions and S-wave travel time curve

STATION	T-O(sec)	STATION	T-O(sec)	STATION	T-O(sec)
1	6.5	11*	4.37	21	14.8
2*	6.90	12*	5.98	22	20.0
3*	2.61	13	6.4	24	4.2
4*	6.12	14	11.0	25	5.3
5*	6.89	15*	6.68	26	4.5
6	6.0	16*	6.98	27	9.8
7*	7.28	17	14.0	28	3.8
8*	9.04	18*	7.95	29	6.5
9	5.0	19*	7.74	31	10.1
10	6.2	20	13.2	32*	5.20

* absolute trigger time available

accelerograms comes from the epicenter. Table 1 presents the trigger time minus the origin time (T-O time) at the stations.

Since the arrival times of distinct phases in horizontal accelerograms are determined in the previous section, the distance L, i.e. location of the source corresponding to the identified distinct phase can be calculated by Eq. (1) under an assumed value of rupture velocity. For a high rupture velocity and to the station located to the rupture direction, a certain passing phenomena of seismic waves could happen; the seismic wave from the i-th fault segment be behind in arrival in comparison with that from the j-th ($i<j$) segment and therefore the location of the source cannot be uniquely calculated from accelerograms. We have ascertained that this phenomena does not ocur at least for a rupture velocity less than 2.5 km/s.

It should be noted that only S-wave distinct phases in horizontal motions are used explicitly in the analysis. Utilization of P-wave distinct phases, or of S-P time of corresponding S and P distinct phases would principally increase the reliability of the multiple event analysis and allow a detailed study of the rupture process. In the accelerograms, the P-wave distinct phases were generally more difficult to identify; since the process time (=the fault length/the rupture velocity) is longer than the S-P travel time from the epicenter to the accelerograph stutions, the P-wave motions in vertical motions were not separated from S-wave motions and they overlapped. Besides this, it appears in many accelerograms that the first P-wave from the epicenter arrived before the trigger time. For these reasons, multiple event analysis using P-wave distinct phases is not made in this study.

4. RESULTS AND DISCUSSION

According to the procedure explained above, the location of the sources corresponding to the distinct phases identified by the visual inspection is uniquely calculated and the results are presented in Fig. 8. Note that the fault is divided into 23 segments of 1.7 km length and that the rupture velocity is assumed to be constant at 2.5 km/sec over the entire fault. The focal depth of 8 km is used. The numbers in Fig. 8 denote the stations whose locations are shown in Fig. 1. For example at the station No. 13, namely, El Centro Array No. 3 (Fig. 1), two distinct phases are identified in the horizontal component of the accelerogram (Fig. 4) and are found, by the computation, to come from the sources at the first (epicenter) and 10 th fault segments, respectively. Note that the distribution shown in Fig. 8 was found not sensitive at least to the rupture velocity V_r= 2.3-2.5 km/s, although the results are not presented herein.

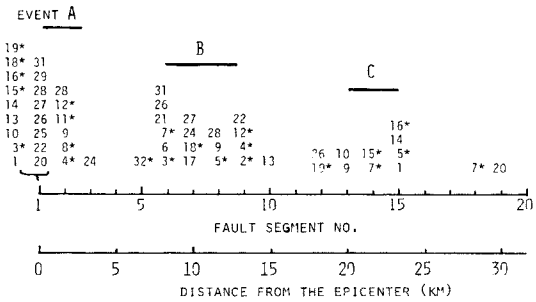

Fig. 8 Distribution of source corresponding to distinct phases on the fault (identified by visual inspection)

Fig. 8 indicates that the 1979 earthquake roughly consists of three events : A, B and C. Many stations identified the event A. This is because the trigger time of accelerograms with no absolute trigger timings was estimated under the assumption that the first S-wave motion arrival is a direct seismic wave from the epicenter. Therefore it cannot be concluded that the large seismic energy is released at the event A. A number of the stations identified the event B locating at the distance 8-13 km from the epicenter. Distinct phase in the middle part of the strong motions would be generally not clearly observed unless its amplitude is fairly large in comparison with that of the preceding motion. Taking this into account, the event B could be the largest event releasing the bulk of seismic energy in the period range of less than 1 to 2 second.

Next, the results by the quantitative method are presented in Fig. 9, where the ordinate is the total score and the abscissa is the distance from the epicenter along the fault. The focal depth is taken to 7 km and the causative fault of 38 km length is divided into 240 segments. Note that the score in each fault segment is the sum of the ranks of distinct phases in the three filtered motions of each accelerograms. The rupture velocity is assumed to be 2.3-2.5 km/s, corresponding to a)-c) in Fig. 9. The total score in Fig. 9. 1) is computed using only the distinct phases with

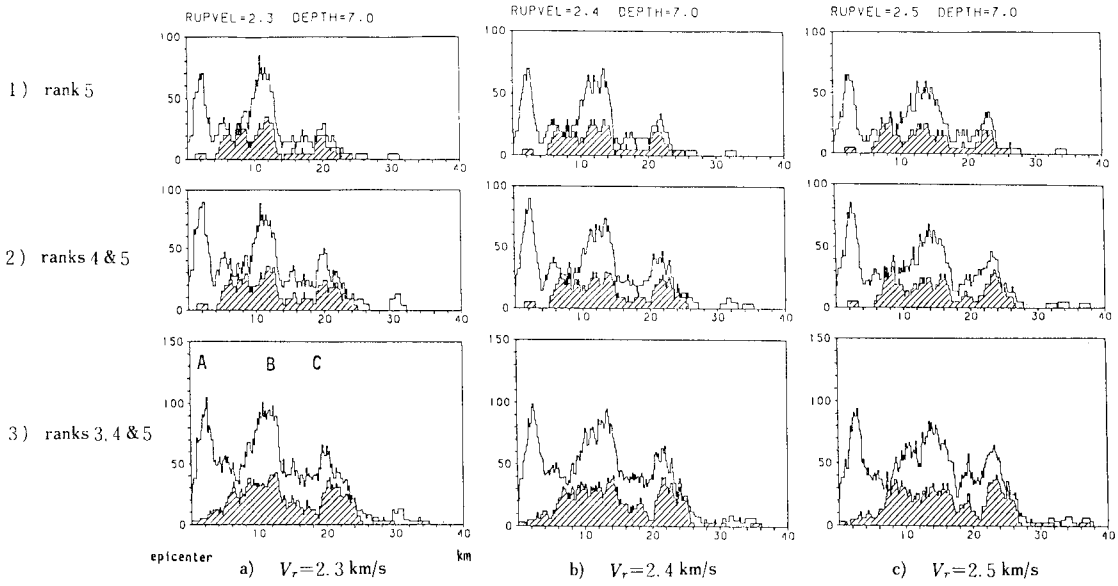

Fig. 9 Distribution of score of distinct phases on the fault for V_r=2.3-2.5 km/s (by quantitative method).

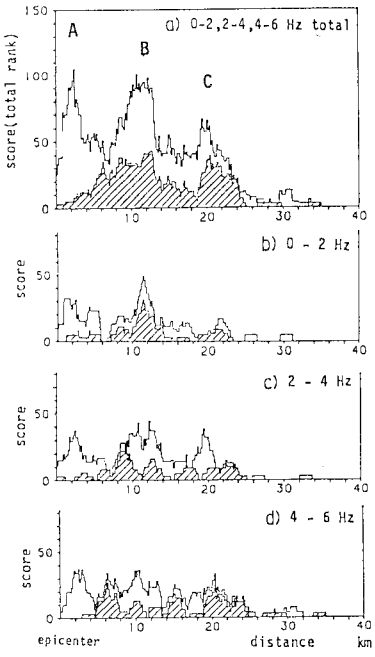

Fig. 10 Distribution of score.

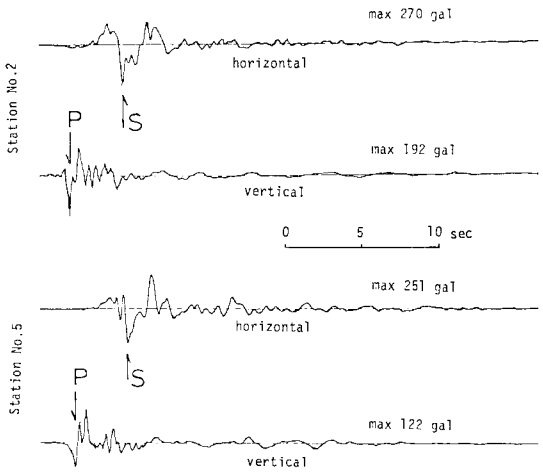

Fig. 11 Corresponding S- and P-distinct phases (0-2 Hz filtered acceleration).

the rank 5, while 2) and 3) are with the ranks 4 and 5, and the ranks 3, 4 and 5, respectively. The score with shade is obtained from the accelerograms with the known absolute timing while the score without shade is from all the accelerograms. Fig. 9 shows that clearly-separated three clusters of high score and a result similar to that in Fig. 8. It should be noted that, since the first S-wave arrival in the acclerograms with no absolute trigger timings were assumed as the direct wave from the epicenter, there is a high sore (no shaded) near the epicenter.

Fig. 10 shows the frequency dependence of the distribution of the total score calculated from the ranks of distinct phases. Note that only the results for the rupture velocity of 2.3 km/sec are presented. In the longer period ground

Table. 2 Rupture velocity and location of event calculated from S- and P-distinct phases (see Fig. 11).

Station	S-P(sec)	Location of Event(km)	V_r(km/sec)
2	3.5	12	2.2
5	3.4	13	2.3
19	5.1	12	2.4

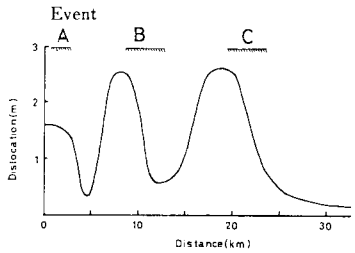

Fig. 12 Dislocation distribution along the fault obtained by Hartzell and Helmberger[3] and location of events A, B and C.

motion (0-2 Hz) the clusters of score, especially at the location of 8～13 km from the epicenter can be observed whereas in shorter period motion (4-6 Hz) total score is rather uniformly distributed. This may indicate that the spatial distribution of generation of seismic waves on a fault is dependent on the frequency range.

Location of the event and rupture velocity can be determined from the S-P time of the distinct phase in the accelerograms of which the trigger time is known. Fig. 11 shows examples of 0-2 Hz band-pass filtered acceleration motions where distinct phases of S and P waves can be clearly identified and are probably from the same event. Table 2 presents the rupture velocity and location of the event calculated from S-P time shown in Fig. 11. This result also suggert that the rupture velocity is approximately 2.3 km/s and furthermore that the event B is located around 12 km from the epicenter.

According to the visual inspection as well as the quantitative criterion, it is found that this earthquake is a multiple event sequence with three events. The event A is located near the epicenter and B is approximately 8～13 km distant from the epicenter while C is located at 18～23 km or so (Figs. 8 and 9). The size of the three events is of engineering concern. Utilizing the work by Kanamori and Jennings[15] and by Luco[16], the average local magnitudes M_L of these three events are calculated from the accelerograms ;

M_L=5.8 for event A
6.3 for event B
6.1 for event C

The local magnitude of this earthquake calculated from the same accelerograms by Luco[16] is 6.3 (average) although the local magnitude reported by USGS is 6.6. Conclusively, the event B is the largest event among the three and released the most of the seismic wave energy of the period less than 1 to 2 secnod.

Hartzell and Helmberger[3] obtained, by the waveform matching method, a two-dimensional fault dislocation model to explain twelve three-component strong-motion displacement records of this earthquake. It should be noted that dominant period of the displacement motion is around 5 second which is longer than the period range considered in this analysis. Their preferred model has two localized areas of larger dislocations as shown in Fig. 12 ; one just north of the border near Bonds Corner (approximately 8 km from the epicenter), a second under Interstate 8 at Meloland Overpass (18 km from the epicenter). Besides the two localized area, there is a small event near the epicenter. Comparing the results in Figs. 8 and 9 with that in Fig. 12, one can find that in both there are three events, but that the events B and C are not completely coincident in location to the localized areas of larger dislocation. They are located rather at the ending part of the localized areas having large dislocation. This implies that large dislocation does not necessarily generate a lage amount of seismic waves of the period less 1 to 2 second. If the portion of the fault than with small dislocation is allowed to be called "barrier", apparently, such short-period seismic waves are mostly generated when the fault rupture approaches the barriers. However, further study has to be conducted to produce a definite conclusion regarding the generation of short-period strong seismic waves on the fault dislocation.

Olson and Aspel[17] also presented slip distribution of the 1979 Imperial Valley earthquake by means of an inverse theory with the low-pass filtered acceleration motions. Their major conclusion is that, although slip is rather

uniformly distributed along the fault, there is a relatively large offset occurring between 15 and 20 km north of the epicenter, which is party in agreement with the Hartzell's result. However, large slip offset around 8 km north of the epicenter is not obtained in Ref. 17). Olson *et al.* assumed bilateral fault rupture in their waveform matching procedure, whereas Hartzell *et al.* and our study employed unilateral rupture. The reasons why the final result in Ref. 17) is noticeably different from that in Ref. 3) and ours are not clear. Since many assumptions and premises in Ref. 3) and this study are common, it is thought Hartzell's result is more suitable for comparison with our result.

5. CONCLUDING REMARKS

An analysis of the multiple rupture process of the 1979 Imperial Valley earthquake is made by identifying distince phases in the near-field horizontal accelerograms. In the identification, visual inspection approach and quantitative approach are employed. It is found that this earthquake is a multiple event with three smaller events, namely A, B and C in the period range of less than 1 to 2 second, indicating that most of the energy was released from the localized areas of the fault.

The event B located at 8～13 km distance from the epicenter has the local magnitude of 6.3 which is almost equal to the local magnitude of this earthquake and is found to be the largest event among the three. The results are compared with the spatial dislocation model obtained by Hartzell and Helmberger[3] and it is found that location of the events A, B and C is not completely coincident to the localized areas having large dislocation. The comparison implies that large amount of short-period seismic waves is generated when the fault rupture approaches the barriers where the dislocation is small. In order to produce a definite conclusion concerning the generation of short period seismic waves during the fault rupture, more detailed study has to be conducted.

6. ACKNOWLEDGMENTS

The authors are grateful to Prof. M. McCann, Jr, Stanford University for his providing us the data of the strong motion recorded in the Northern Baja Network. The research was in part supported by Grant-in-Aid from the Japanese Ministry of Education, Science and Culture.

REFERENECES

1) Fujino, Y. *et al.* : Identification of multiple rupture process of 1979 Imperial Valley earthquake by near-field accelerograms, Proc. of sixth Japan Earthquake Engineering Symposium, pp. 97～104, 1982.
2) Fujino, Y., *et al.* : Mutiple event analysis of 1979 Imperial Valley earthquake using distinct phases in near-field accelerograms, Proc. of Review Meeting of US-Japan Coop. Res. on Seismic Risk and Its Use in Code Formulation, pp. 1～9, Mar., 1983.
3) Hartzell, S. and Helmberger, D. V. : Strong-motion modeling of the Imperial Valley earthquake of 1979, BSSA, Vol. 72, No. 2, pp. 571～596, 1982.
4) Matthiesen, R. B. and Porcella, R. L. : Strong-motion data summary, Imperial valley earthquake of October 15, 1979 and aftershocks, CIRC 818-C, U. S. Geol. Sury., pp. 3～17, 1981.
5) Kanamori, H. and Stewart, G. S. : Seismological aspects of the Guatemala earthquake of February 4, 1976, J. Geophys. Res. Vol. 83, pp. 3427～3434, 1978
6) Kikuchi, M. and Kanamori, H. : Inversion of complex body waves, BSSA., Vol. 72, No. 2, pp. 491～506, 1982.
7) Fukao, Y. and Furumoto, M. : Foreshocks and multiple shocks of large earthquakes, Physics of the Earth and Planetary Interiors, No. 10, pp. 355～368, 1975.
8) Seno, T. *et al.* : Rupture process of the Miyagi-oki, Japan, earthquake of June 12, 1979, Physics of the Earth and Planetary Interiors, No. 23, pp. 39～61, 1980.
9) Trifunac, M. D. and Brune, J. N. : Complexity of energy release during the Imperial Valley California, earthquake of 1940 BSSA, Vol. 60, No. 1, pp. 137～160, 1970.
10) Archuleta, R. J. : Analysis of near-source static and dynamic measurements from the 1979 Imperial valley earthquake, BSSA, Vol. 72, No. 6, pp. 1927～1956, 1982.
11) Brady, A. G., Perez, V. and Mork, P. N. : The Imperial valley earthquake, October 15, 1979 (Digitalization and processing of accelerograph records), U. S. Geol. Surv. Open-File Report 80-703, 1980.
12) Nagamune : Process in the source region for a great earthquake, J. Seism. Soc. Japan, Vol. 22, No. 2, pp. 104～114, 1969 (in Japanese).

13) Fuis, G. S. *et al.* : Crustal structure of the Imperial valley region, U. S. Geol. Sury. Profess. Paper 1254, 1982.
14) Saito, M. : An automatic design algorithm for band selective recusive digital filters, Geophysical Exploration, Vol. 31, No. 4, pp. 112～135, 1978 (in Japanese).
15) Kanamori, H. and Jennings, P. C. : Determination of local magnitude M_L from strong-motion accelerograms, BSSA, Vol. 61, No. 2, pp. 1073～1095, 1978.
16) Luco, J. E. : A note on near-source estimates of local magnitude, BSSA, Vol. 72, No. 3, pp. 941～958, 1982.
17) Olson, A. H. and Aspel, R. J. : Finite faults and inverse theory with applications to the 1979 Imperial Valley earthquake, BSSA, Vol. 72, No. 6, pp. 1969～2001, 1982.

(Recieved December 16, 1983)